

Enhanced magnetic property of Mn-doped BiFeO₃ nanowires fabricated by electrospinning

Geon Myeon Bak, Chan-Geun Song and Jong-Won Yoon*

Department of Materials Science and Engineering, Dankook University, Cheonan, Chungnam 31116, Korea

One-dimensional BiFe_{1-x}Mn_xO₃ (x = 0 and 0.05) nanowires were prepared by electrospinning method to study the effects of Mn substitution on their crystal structure, particulate size, and magnetic properties. X-ray diffraction studies revealed a structural phase transitions from rhombohedral to orthorhombic with Mn-doping. Transmission electron microscopy (TEM) images revealed that the nanofibers were composed of fine particulates with diameter of about 55 ± 5 nm in pure BiFeO₃ and 40 ± 5 nm in 5 mole% Mn-doped BiFeO₃ nanowires. The chemical state of Mn³⁺ and Mn⁴⁺ in Mn-doped BiFeO₃ nanowires were confirmed by X-ray photoelectron spectroscopy (XPS) measurement. The magnetic hysteresis loops indicate soft ferromagnetic behavior in pure BiFeO₃ and 5 mole% Mn-doped BiFeO₃ nanowires. With 5 mol% Mn doping in BiFeO₃ nanowires, remnant magnetization increased from 0.279 to 0.378 emu/g at 10 K which is attributed to the structural phase transition from rhombohedral to orthorhombic phase and reduction of particulate size.

Keywords: Mn-doped BiFeO₃ nanowires, Electrospinning, TEM, XPS, Magnetic property.

Introduction

Multiferroic materials showing simultaneous coupling of ferroelectricity and ferromagnetism have recently attracted considerable attention due to their potential applications and attractive physical phenomena [1-4]. BiFeO₃ is known to be the only material that has both ferroelectric ($T_C \sim 1103$ K) and antiferromagnetic ($T_N \sim 643$ K) properties at room temperature, which makes it an excellent possible candidate for actual multiferroic applications [5, 6]. However, BiFeO₃ is a highly metastable compound and it is difficult to prepare impurity-free phase of BiFeO₃, due to easily volatile Bi atoms [7]. Also, BiFeO₃ has a spiral spin structure with a lengthy spiral period ~ 62 nm, which superimposes on the antiferromagnetic ordering and results in the cancellation of net magnetization [8,9]. Park et al. reported that BiFeO₃ nanoparticles exhibited a ferromagnetic characteristics with different particles size [10].

Several research groups have tried A-site (Bi-site) and B-site (Fe-site) substituting to modify the multiferroic properties of BiFeO₃ in recent years [11, 12]. The incorporation of rare-earth cations in BiFeO₃ seems to increase the magnetocrystalline anisotropy, thus making the cycloidal spin structure energetically unfavourable [6]. Singh et al. suggested that La³⁺ substitution for Bi³⁺ eliminates impurity phases along with a structural phase transition improving the magnetic properties [13]. Liu et al., in their investigations of Ce-doped BiFeO₃ thin

films, reported a change in the crystal structure of the material which resulted in improved the magnetic properties [14]. With Mn doping transition metals in BiFeO₃ nanopowders, a few studies related with magnetic property were carried out [15].

Electrospinning method is easy and simple process to fabricate nanowires with nano-sized diameter. To fabricate ceramic nanofibers, there are only three steps; first of all a sol solution which has viscosity is required. And then an electrical potential is applied to a droplet of the sol solution. When the applied electric field exceeds the surface tension of the droplet, it starts to fabricate nanowires from the droplet. As-spun nanofibers are collected on a grounded metal plate. Finally, polymers and residual solvent is flied off, and the nanowires are crystallized by calcination. For a very short time, tens of nanometers linear nanofibers can be prepared by electrospinning [16-19]. In this study, we concentrate on fabricating pure BiFeO₃ and 5 mol% Mn-doped BiFeO₃ nanowires. The starting materials, electrospinning conditions, and heat-treatment conditions were different with our previous reports. The aim of this study is to fabricate Mn-doped BiFeO₃ nanowires by electrospinning and to clarify the relationship between the phase transition with Mn doping and the magnetic properties.

Experimental Procedure

Electrospinning technique were used to fabricate BiFe_{1-x}Mn_xO₃ (x = 0, 0.05) nanowires. The sol solution was made with bismuth (III) nitrate pentahydrate (1.680 g), iron (III) nitrate nonahydrate (1.340 and 1.27 g for 0 and 5 mol%, respectively), and a desired

*Corresponding author:
Tel : +82-41-550-3536
Fax: +82-41-569-2240
E-mail: jwoon@dankook.ac.kr

at.% of manganese (II) nitrate tetrahydrate (0 and 0.042 g for 0 and 5 mol%, respectively) was dissolved in N,N-dimethylformamide (10 ml) and polyvinylpyrrolidone (PVP, MW = 1,300,000) (2 g) dissolved in the solution while stirring for one hour to obtain optimized viscosity.

A nanofiber electrospinning unit purchased from Nano NC Co., Ltd. (South Korea) was used to prepare $\text{BiFe}_{1-x}\text{Mn}_x\text{O}_3$ ($x = 0, 0.05$) nanowires. The $\text{BiFe}_{1-x}\text{Mn}_x\text{O}_3$ precursor solution was loaded into a 10 ml syringe with a 0.15 mm diameter stainless-steel needle. A grounded aluminium foil served as a counter electrode and collector plate. $\text{BiFe}_{1-x}\text{Mn}_x\text{O}_3$ ($x = 0.00$ and 0.05) nanowires were synthesized by applying 10 kV to the solution through the needle tip. The distance between the needle tip and collector was fixed at 15 cm. Electrospinning experiments were performed at room temperature with a relative air humidity of 40–45%. As-spun $\text{BiFe}_{1-x}\text{Mn}_x\text{O}_3$ nanowires were calcined at 500 °C in air for 20 min with a heating rate of 2.5 °C/min.

The morphologies of the samples were further observed by transmission electron microscopy (TEM) and high resolution transmission electron microscopy (HRTEM) investigation by Jeol ARM1300S. Scanning electron micrographs were obtained using a LEO 1455VP (Carl Zeiss, Germany). High voltage electron microscope (HVEM) operated at an accelerating voltage of 1200 kV. The crystal structure of the $\text{BiFe}_{1-x}\text{Mn}_x\text{O}_3$ nanofibers was characterized by X-ray diffraction measurements using a X'Pert Powder, PANalytical X-ray diffractometer (Netherlands) with Cu K_α radiation ($\lambda = 0.154$ nm) operated at 40 kV and 30 mA. The crystal structure was refined by the Rietveld method and Jade software was used to identify the impurity peaks. Measurement of magnetization versus temperature was recorded on a home-made unit VSM (vibrating sample magnetometer), using lock-in-amplifier model 5210 (USA) with temperature controller Oxford ITC 503. The magnetization curves were also measured by the magnetic property measurement system (MPMSTM, Quantum Design).

Results and Discussion

Fig. 1(A) shows XRD patterns of pure BiFeO_3 and 5 mol% Mn-doped BiFeO_3 nanowires calcined in air at 500 °C with holding time of 20 min. The results indicate that BiFeO_3 nanowires had a perovskite-based rhombohedral structure (JCPDF no. 86-1518) with a small amount of impurity. The impurity peaks can be found easily due to volatile Bi atoms [20,21]. Fig. 1(B) represents a magnified XRD pattern around $2\theta = 32^\circ$ of Fig. 1(A). As shown in this fig, (104) and (110) peaks are clearly separated in the pure BiFeO_3 nanowires. In case of 5 mol% Mn-doped BiFeO_3 nanowires, the doublet peaks merge to a single (110) peak. This result suggests small lattice distortion from the rhombohedral structure of

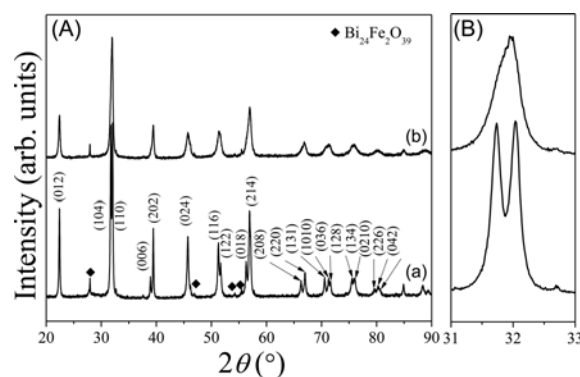


Fig. 1. (A) XRD patterns of Mn-doped LaFeO_3 nanofibers; (a) pure BiFeO_3 and (b) 5 mol% Mn-doped BiFeO_3 nanowires. (B) Enlarged XRD patterns in the vicinity of $2\theta = 32^\circ$.

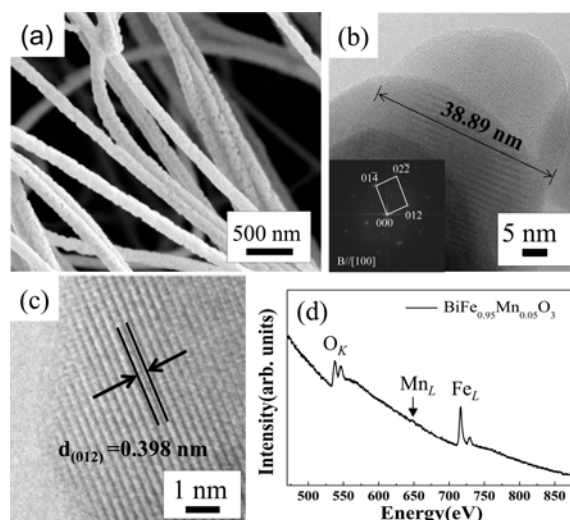


Fig. 2. (a) FE-SEM image, (b) HR-TEM image, (c) HR-TEM image at high magnification and (d) EELS spectrum for 5 mole% Mn-doped BiFeO_3 nanowires.

BiFeO_3 with Mn doping. Similar behavior has been reported in Mn-doped BiFeO_3 film, which corresponds to a lattice distortion or phase change from rhombohedral to orthorhombic [22]. The average crystallite sizes of the Mn-doped BiFeO_3 nanowires were calculated using Scherrer's formula. The average crystallite size decreases with 5 mol% Mn doping in BiFeO_3 nanowires from 55.34 nm to 40.52 nm. The crystallite or grain size of materials depends on the diffusivity of the individual grains, sintering temperature and porosity [23, 24]. Thus crystallite-size decrease in the Mn-doped BiFeO_3 nanofibers is most likely caused by reduced chemical diffusivity associated with the Mn substitution.

The morphologies of the pure and Mn-doped samples characterized by FE-SEM and HR-TEM. Representative FE-SEM images for 5 mole% Mn-doped BiFeO_3 nanowires are presented in Fig. 2(a). The 5 mole% Mn-doped BiFeO_3 nanowires showed relatively homogeneous distribution with a diameter about 200–300 nm. Figs. 2(b) and (c) show typical HR-TEM images of the 5 mole% Mn-doped BiFeO_3 nanowires at different magnifications.

The inset of Fig. 2(b) shows a SAED pattern. Fig. 2(b) shows that a single nanowire was composed of several nanoparticulates with average diameter of about 38 ± 5 nm. It can be noticed that the crystallite sizes calculated via Scherrer's formula from XRD measurements are in good agreement with nanoparticulates sizes observed by TEM. As confirmed by the clear lattice image of Fig. 2(c) at high magnification, the sample consisted of single crystal particles with high crystallinity. Fig. 2(d) displays EELS spectrum of Mn-doped BiFeO₃ nanowires, which confirms the presence of Fe, O, and Mn elements.

The surface composition and chemical states of pure BiFeO₃ and 5 mol% Mn-doped BiFeO₃ nanowires were examined by XPS. Fig. 3(A) shows XPS spectra of Mn 2p. In pure BiFeO₃ nanowires, no Mn 2p peaks were found (Fig. 3A(a)), whereas Mn 2p peaks were observed in Mn-doped BiFeO₃ nanowires (Fig. 3A(b)). This result is in good agreement with the EELS result. It has been known that the peak position is concentrated at 641.7–642.0 eV for Mn³⁺ and 643.2 eV–644.0 eV for Mn⁴⁺ [25–27]. Therefore, an asymmetric broadband observed near the Mn 2p_{3/2} spectra implies that there is the coexistence of Mn³⁺ and Mn⁴⁺ in Mn-doped BiFeO₃. The binding energy of Fe 2p_{3/2} and Fe 2p_{1/2} is 710.4 eV and 724.2 eV, as seen Fig. 3(B). Also, a satellite peak exists between Fe 2p_{3/2} and Fe 2p_{1/2} peaks at 718.4 eV. It means that chemical state of Fe ion mainly exists as Fe³⁺ of pure BiFeO₃ and 5 mol% Mn-doped BiFeO₃ nanowires [28]. The Fe 2p_{3/2} peaks were subjected to curve fitting by Gaussian-Lorentzian. The coexistence of Fe³⁺ and Fe²⁺ ions in the BiFeO₃ nanowires is observed. The computed Fe²⁺ contents of pure BiFeO₃ and 5 mol% Mn-doped BiFeO₃ nanowires are 38.3% and 37.5%, respectively. This result could be evidence of the decrease oxygen vacancies in 5 mol% Mn-doped BiFeO₃ nanowires even within the error range.

Fig. 4(a) shows the M-H curves for pure BiFeO₃ and 5 mol% Mn-doped BiFeO₃ nanowires at 10 K. The magnetic hysteresis (M-H) loops indicate soft ferromagnetic behavior in both samples. With 5 mol% Mn doping in BiFeO₃ nanowires, remnant magnetization increased from 0.279 to 0.378 emu/g and coercivity decreased from 124.7 to 87 Oe. In the case of specimens measured at room temperature, remnant magnetization increased from 0.115 to 0.144 emu/g and coercivity decreased from 46.5 to 17.1 Oe as shown in Fig. 4(b). The origin of spontaneous magnetization is due to nano range crystallite size. The helical order in nanocrystals can be well suppressed through decreasing the particle size. It has already been theoretically calculated that, suppression of helical order, with a periodicity about 62 nm on canted antiferromagnetic order between successive (111) ferromagnetic planes, might have resulted in higher magnetization [10]. The increased remnant magnetization in 5 mol% Mn doping in BiFeO₃ nanowires may be attributed to the structural phase transition from

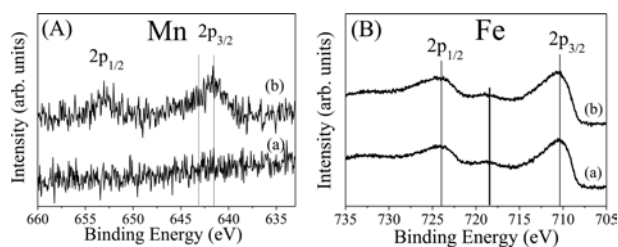


Fig. 3. (A) XPS spectra of the Mn 2p; (a) pure BiFeO₃ and (b) 5 mol% Mn-doped BiFeO₃ nanowires. (B) XPS spectra of the Fe 2p; (a) pure BiFeO₃ and (b) 5 mol% Mn-doped BiFeO₃ nanowires.

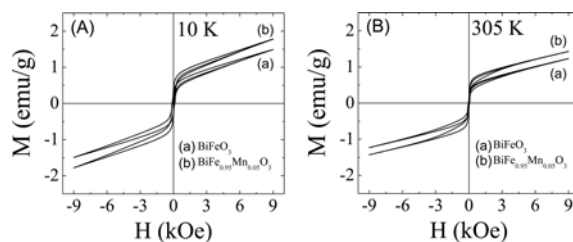


Fig. 4. M-H curves for Mn-doped LaFeO₃ nanofibers measured at (A) 10 K and (B) 300 K; (a) pure BiFeO₃ and (b) 5 mol% Mn-doped BiFeO₃ nanowires.

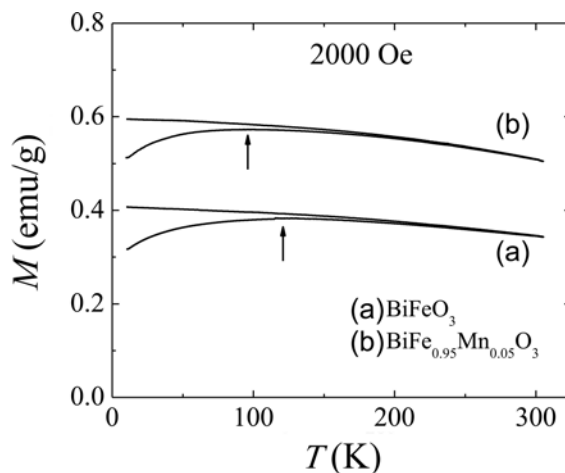


Fig. 5. The ZFC and FC curves measured under magnetic field of 2000 Oe; (a) pure BiFeO₃ and (b) 5 mol% Mn-doped BiFeO₃ nanowires.

rhombohedral to orthorhombic phase and reduction of particulate size. For single domain antiferromagnetic particles, the magnetization is expected to scale as $\sim 1/d$ (where d is the diameter of the particle), that is, as the surface to volume ratio [29]. It is already described in the XRD and TEM result section that the particulate size decreases with Mn doping. From Herzer's report [30], the coercivity decreased with decreasing of particles size above critical particle size. Also, Mn³⁺ and Mn⁴⁺ were observed in the 5 mol% Mn-doped BiFeO₃ nanowires from XPS analysis. Thus the increase of magnetization of BiFeO₃ nanowires with Mn doping is due to the structural phase transition, the decreasing of particulate size.

Fig. 5 displays the ZFC and FC curves measured under magnetic field of 2000 Oe. For pure BiFeO₃ and 5 mol%

Mn-doped BiFeO₃ nanowires, a peak related to spin-glass-like freezing temperature can be observed at about 123.1 and 95.8 K, respectively. The results were very similar to those reported for size-controlled BiFeO₃ nanoparticles [10]. The observed freezing temperatures, such as spin glass, are due to the complex interactions between the finite size effect and the random distribution of anisotropy in BiFeO₃ nanofibers [31]. From the results of M-H and ZFC-FC, the Mn doping of the BiFeO₃ nanowires improves the residual magnetization and coercive force depending on the phase transition from rhombohedral structure to orthorhombic structure and particle size. Thus, our work demonstrates that Mn doping in BiFeO₃ nanowires is very effective in controlling magnetism through particle size control and should be useful in electromagnetic device applications

Conclusions

One-dimensional BiFe_{1-x}Mn_xO₃ (x = 0 and 0.05) nanowires were successfully fabricated by electrospinning and subsequent calcination for a short time of the as-spun nanowires. Phase transformation was confirmed from rhombohedral structure to orthorhombic structure. The particulate size decreased from 55 to 40 nm with 5 mole% Mn doping. The chemical state of Mn³⁺ and Mn⁴⁺ in Mn-doped BiFeO₃ nanowires were observed. With 5 mol% Mn doping in BiFeO₃ nanowires, remnant magnetization increased from 0.279 to 0.378 emu/g at 10 K which is mainly attributed to the structural phase transition from rhombohedral to orthorhombic phase and reduction of particulate. The coercivity is decreased from 124.7 to 85.6 Oe, following an increasing trend with increase of particles size up to a critical particle size.

Acknowledgments

This study was conducted by the research fund of Dankook University in 2015.

References

1. M. Fiebig, *J. Phys. D: Appl. Phys.* 38 (2005) R123-R152.
2. C.W. Nan, M. I. Bichurin, S. Dong, D. Viehland and G. Srinivasan, *J. Appl. Phys.* 103 (2008) 031101.
3. K.F. Wang, J.-M. Liu and Z. F. Ren, *Adv. Phys.* 58 (2009) 321-448.
4. W. Eerenstein, N.D. Mathur and J.F. Scott, *Nature* 442 (2006) 759-765.
5. J. Wang, J.B. Neaton, H. Zheng, V. Nagarajan, S.B. Oqale, B. Liu, D. Viehland, V. Vaithyanathan, D.G. Schlom, U.V. Waghmare, N.A. Spaldin, K.M. Rabe, M. Wuttig and R. Ramesh, *Science* 299 (2003) 1719-1722.
6. X. Zhang, Y. Sui, X. Wang, Y. Wang and Z. Wang, *J. Alloys Comp.* 507 (2010) 157161.
7. D.S. Kim, J.S. Kim and C.I. Cheon, *J. Korean Ceram. Soc.* 53 (2016) 162-166.
8. I. Sosnowska, T.P. Neumaier and E. Steichele, *J. Phys. C: Solid State Phys.* 15 (1982) 4835-4846.
9. C. Ederer and N.A. Spaldin, *Phys. Rev. B* 71 (2005) 060401.
10. T.J. Park, G.C. Papaefthymiou, A.J. Viescas, A.R. Moodenbaugh and S.S. Wong, *Nano Lett.* 7 (2007) 766-772.
11. J.W. Woo, S. B. Baek, T.K. Song, M.H. Lee, J. Rahman, W.-J. Kim, Y.S. Sung, M.-H. Kim and S. Lee, *J. Korean Ceram. Soc.* 54 (2017) 323-330.
12. J.-H. Jeong, C.-G. Song, K.-H. Lee, W. Sigmund and J.-W. Yoon, *J. Alloys Comp.* 749 (2018) 599-604.
13. V.R. Singh, A. Garg and D.C. Agrawal, *Appl. Phys. Lett.* 92 (2008) 152905.
14. Z. Quan, W. Liu, H. Hu, S. Xu, B. Sebo, G. Fang, M. Li and Z. Zhao, *J. Appl. Phys.* 104 (2008) 084106.
15. S. Chauhan, M. Kumar, S. Chhoker, S.C. Katyal, H. Singh and M. Jewariya, *Solid State Comm.* 152 (2012) 525-529.
16. K. W. Lee, K.S. Kumar, G. Heo, M.-J. Seong and J.-W. Yoon, *J. Appl. Phys.* 114 (2013) 134303.
17. T. Moon, W.-Y. Lee, C.-J. Choi and J.-W. Yoon, *Appl. Phys. Lett.* 105 (2014) 153103.
18. C.-M. Tsai, C.-G. Song, Y.-C. Hung, Y.-G. Jeong, S.H. Oh, J.H. Jeong, H. Huh, J.-W. Yoon and W. Sigmund, *Ceram. International* 43 (2017) 3761-3768.
19. W.Y. Lee, H.J. Yun and J.-W. Yoon, *J. Alloys Comp.* 583 (2014) 320-324.
20. D. Kothari, R.V. Raghavendra, A. Gupta, D.M. Phase, N. Lakshmi, S.K. Deshpande and A.M. Awasthi, *J. Phys.: Condens. Matter* 19 (2007) 136202.
21. S. Iakovlev, C.-H. Solterbeck, M. Kuhnke and M. Es-Souni, *J. Appl. Phys.* 97 (2005) 094901.
22. S.K. Singh, H. Ishiwara and K. Maruyama, *Appl. Phys. Lett.* 88 (2006) 262908.
23. A.C.F.M. Costa, E. Tortella, M.R. Morelli and R.H.G.A. Kiminami, *J. Magn. Magn. Mater.* 256 (2003) 174-182.
24. J. Kim, J.H. Ha, J. Lee and I.H. Song, *J. Korean Ceram. Soc.* 54 (2017) 331-339.
25. R.J. Iwanowski, M.H. Heinonen and E. Janik, *Chem. Phys. Lett.* 387 (2004) 110-115.
26. Y. Umezawa and C.N. Reilly, *Anal. Chem.* 50 (1978) 1290-1295.
27. S.R.S. Kumar, M.N. Hedhili, H.N. Alshareef and S. Kasiviswanathan, *Appl. Phys. Lett.* 97 (2010) 111909.
28. G. Dong, G. Tan, W. Liu, A. Xia and H. Ren, *J. Mater. Sci. Technol.* 30 (2014) 365-370.
29. J.T. Richardson, D.I. Yiagas, B. Turk, K. Forster and M.V. Twigg, *J. Appl. Phys.* 70 (1991) 6977.
30. G. Herzer, *IEEE Transac. Magn.* 26 (1990) 1397-1402.
31. I. Sonowaska, W. Schäfer, W. Kochelmann, K.H. Anderson and I.O. Troyanchuk, *Appl. Phys. A* 74 (2002) S1040-S1042.